## Supplementary Information

### Supplementary Methods

*Hematoxylin and eosin (HE) staining*

Prepared sections of various organs and tissues of mice were individually dewaxed in xylene three times for 20 min, sequentially soaked in 100% ethanol for 5 min, 95% ethanol for 5 min, 80% ethanol for 5 min, and three times in PBS for 5 min. Stained with hematoxylin for 5 min, washed with tap water for 1 min, 1% hydrochloric acid alcohol solution for 10 s, and once again with tap water for 1 min, then distilled water for 15 min. Finally, after soaking in 0.5% eosin dye for 2 min and rinsing with water for 2 min, the dehydrated slices were observed under an optical microscope.

### Supplementary Results

### Supplementary Figure 1

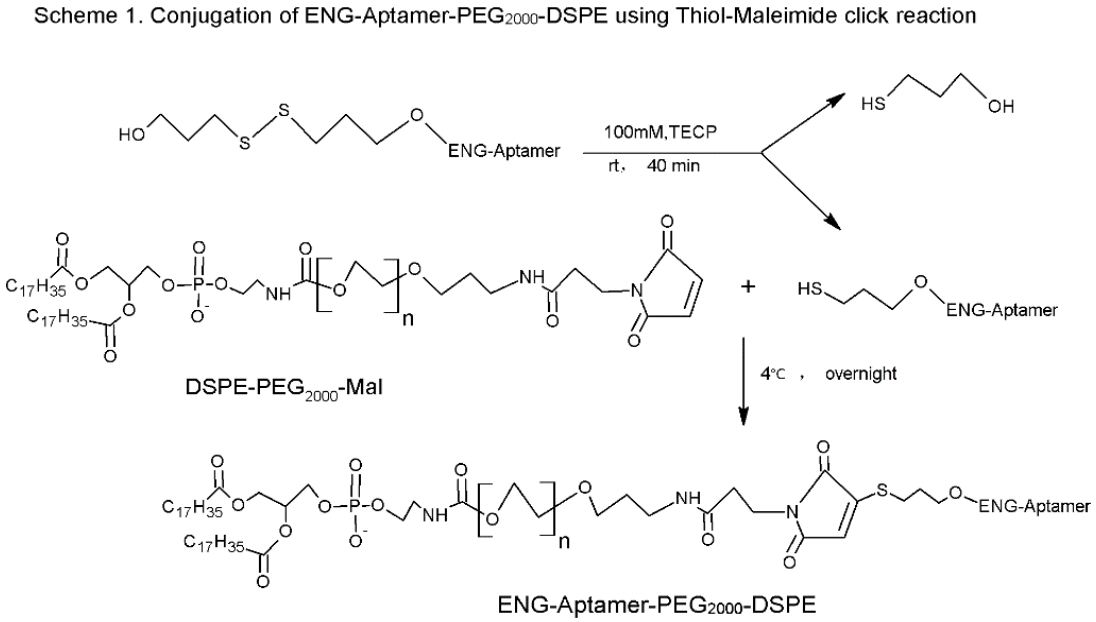


**Supplementary Figure 1: Conjugation of ENG-Aptamer-$PEG_{2000}$-DSPE using Thiol-Maleimide click reaction.**

1:5 ratio of ENG-aptamer sequence and maleimide-$PEG_{2000}$-DSPE was incubated at 4 °C under $N_2$ for 24 h in darkness to obtain ENG-Aptamer-$PEG_{2000}$-DSPE.

**Supplementary Figure 2**

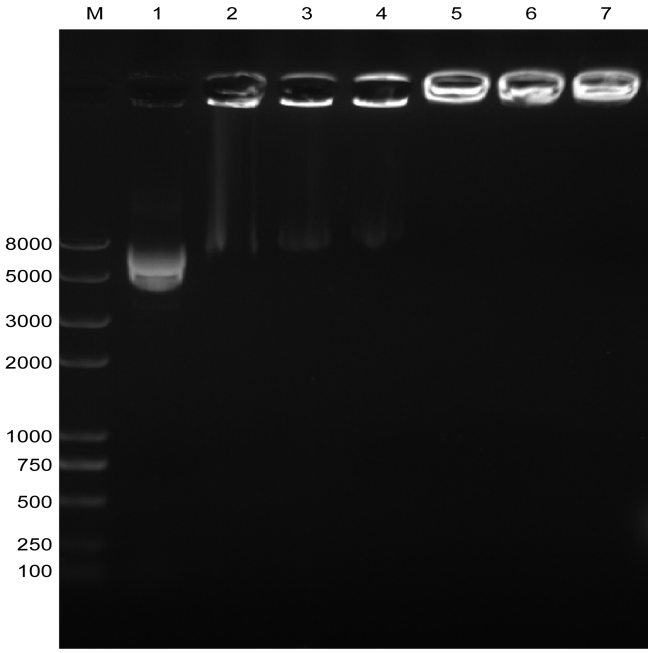


**Supplementary Figure 2: Nitrogen/phosphate(N/P) ratio optimization shown by 1% agarose gel electrophoresis.** 80 μg, 40 μg, 20 μg, 10 μg, and 5 μg plasmids were respectively set in 5 of 100 μL blank LP tubes, then ENG-Apt/mIP-10-LP with a N/P ratio of 1:4, 1:2, 1:1, 2:1, and 4:1, were respectively added. **M:** marker, **Lane 1:** GV143 mIP-10, **Lane 2-7:** ENG -Apt/mIP-10-LP at different N/P ratios (1:4, 1:3, 1:2, 1:1, 2:1 and 4:1).

**Supplementary Figure 3**

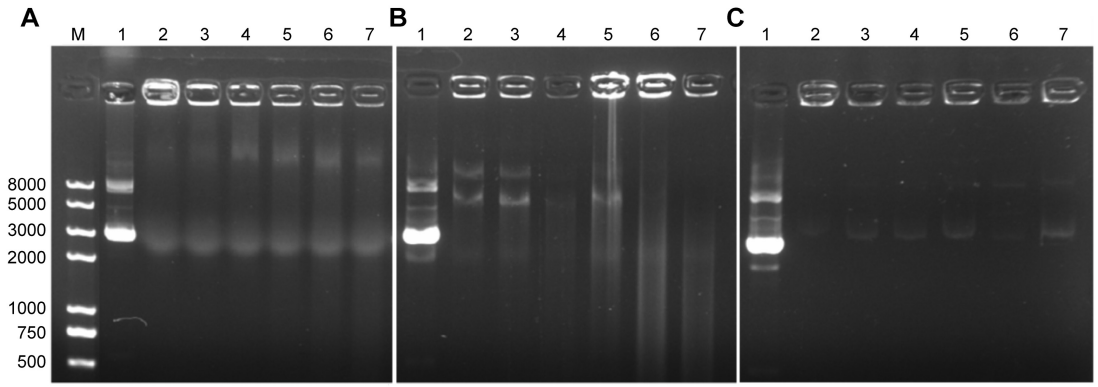


**Supplementary Figure 3: ENG-Apt/mIP-10-LP nanoparticles stability.**

ENG-Apt/mIP-10-LP (20 μL) was respectively added into high-glucose DMEM medium alone, 100% human serum, or high glucose DMEM containing 20% fetal bovine serum, with an incubation time frame of 10 min, 0.5 h, 2 h, 4 h, 6 h, 8 h. In accordance with DNA Marker, mIP-10 plasmid was incubated with three kinds of culture media for 10 min, 0.5 h, 2 h, 4 h, 6 h, 8 h, in this order. **A:** DMEM alone: ENG-Apt/mIP-10-LP at 37 °C in DMEM and observed for 10 min, 0.5 h, 1.5 h, 4 h, 6 h and 8 h showing almost zero plasmid release. **B:** human serum: ENG-Apt/mIP-10-LP at 37 °C in human serum for 10 min, 0.5 h, 1.5 h, 4 h, 6 h and 8 h showing a similar small plasmid release. **C:** high glucose DMEM containing 20% FBS: ENG-Apt/mIP-10-LP at 37 °C in 20% FBS high glucose DMEM for 10 min, 0.5 h, 1.5 h, 4 h, 6 h and 8 h showing low plasmid release.

**Supplementary Figure 4**

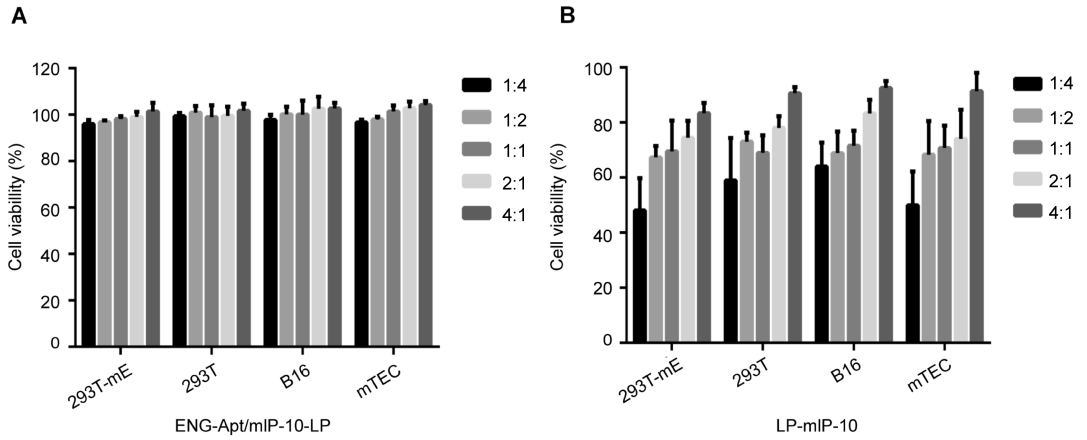


**Supplementary Figure 4: Cytotoxicity of ENG-Apt/mIP-10-LP and LP-mIP-10 at different N/P ratios. A:** Cytotoxicity of ENG-Apt/mIP-10-LP at different N/P ratios (1:4, 1:2, 1:1, 2:1, and 4:1). **B:** Cytotoxicity of LP-mIP-10 at different N/P ratios (1:4, 1:2, 1:1, 2:1, and 4:1). The mean ± SE of three independent experiments is shown.

**Supplementary Figure 5**

293T-mE cells presenting strong fluorescence after FITC/DiI-labeled ENG-Apt/mIP-10-LP nanocapsules culture, in contrast 293T cells presenting weak fluorescence. Similarly, significantly decreased fluorescence of 293T-mE cells covered with excess unlabeled ENG-Aptamer. Fluorescence intensity of 293T-mE cells cultured with DiI-labeled ENG-Apt/mIP-10-IP was significantly higher compared to that of 293T cells, indicating superiorl internalization of ENG-Apt/mIP-10-LP nanocapsules into 293T-mE cells.

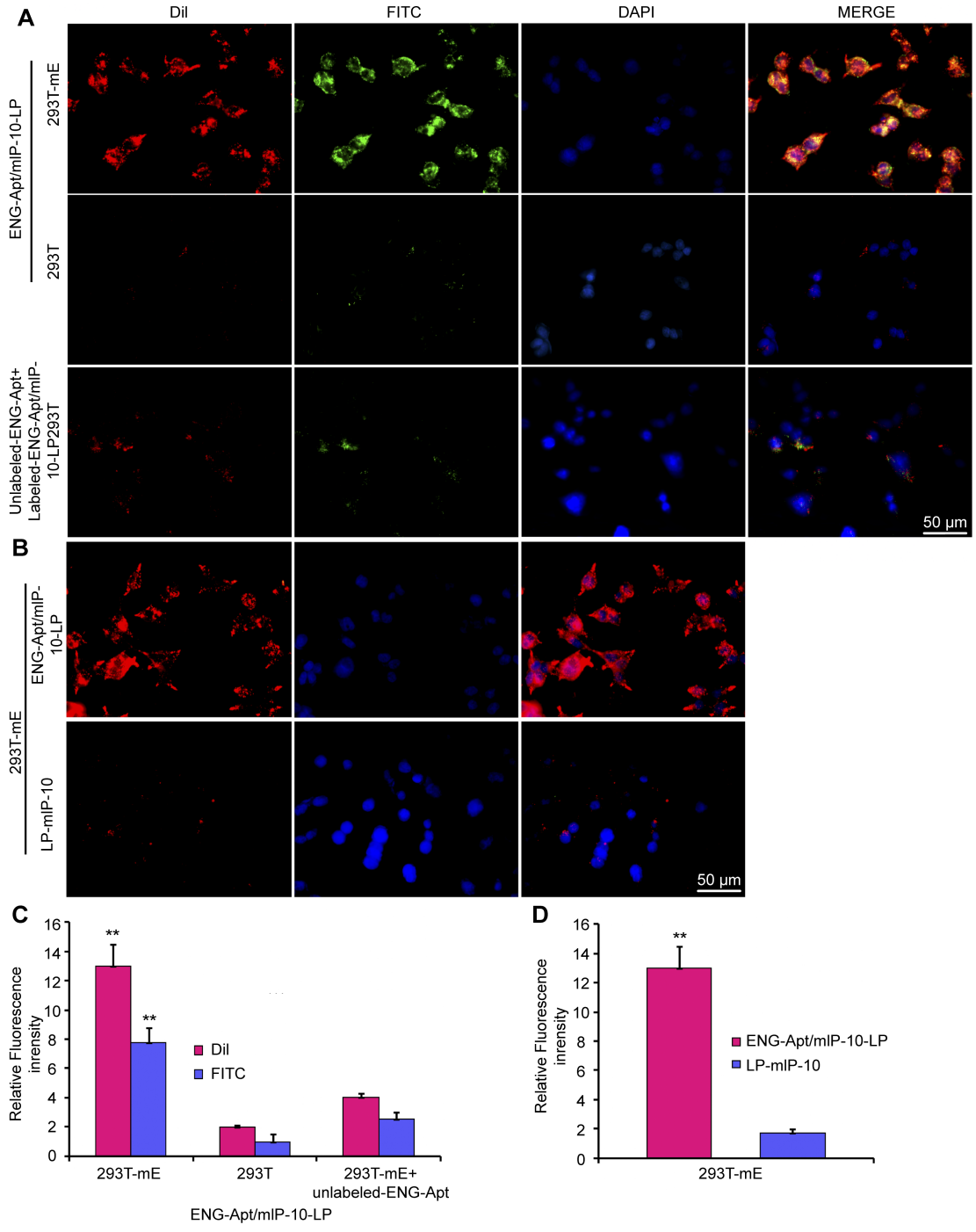

**Supplementary Figure 5: Targeting specificity of ENG-Apt/mIP-10-LP to CD105-positive cells. A, B:** ENG-Apt/mIP-10-LP nanocapsules specifically bind to 293T-mE through ENG receptors as is evident by the fluorescence of DiI-labeled liposomes (red), DAPI-stained nuclei (blue), and FITC-labeled ENG-Aptamer (green), at a magnification of 400×. **C:** the fluorescence intensity analysis in 293T-mE and 293T after binding of ENG-Apt/mIP-10-LP nanocapsules. **D:** the fluorescence intensity analysis in 293T-mE after binding of ENG-Apt/mIP-10-LP nanocapsules is much greater than that with mIP-10-LPs. The mean ± SE of three independent experiments is shown. ** $p < 0.01$ for the comparison of ENG-Apt/mIP-10-LP group to control groups.

**Supplementary Figure 6**

ENG-Apt/mIP-10-LP increased IP-10 expression in mTEC and 293T-mE cells (Figure S6A). Flow cytometric analysis showed that the expression efficiencies in mTEC and 293T-mE cells transfected with ENG-Apt/mIP-10-LP nanocapsules were 62% and 78.6%, respectively, and these efficiencies were significantly higher than the 17% and 26.7% for these cells transplanted with non-targeting mIP-10-LPs. In comparison, the efficiencies with Lipofectamine 2000 were 71.5% and 84.3%, respectively, as shown in Figure S6B.

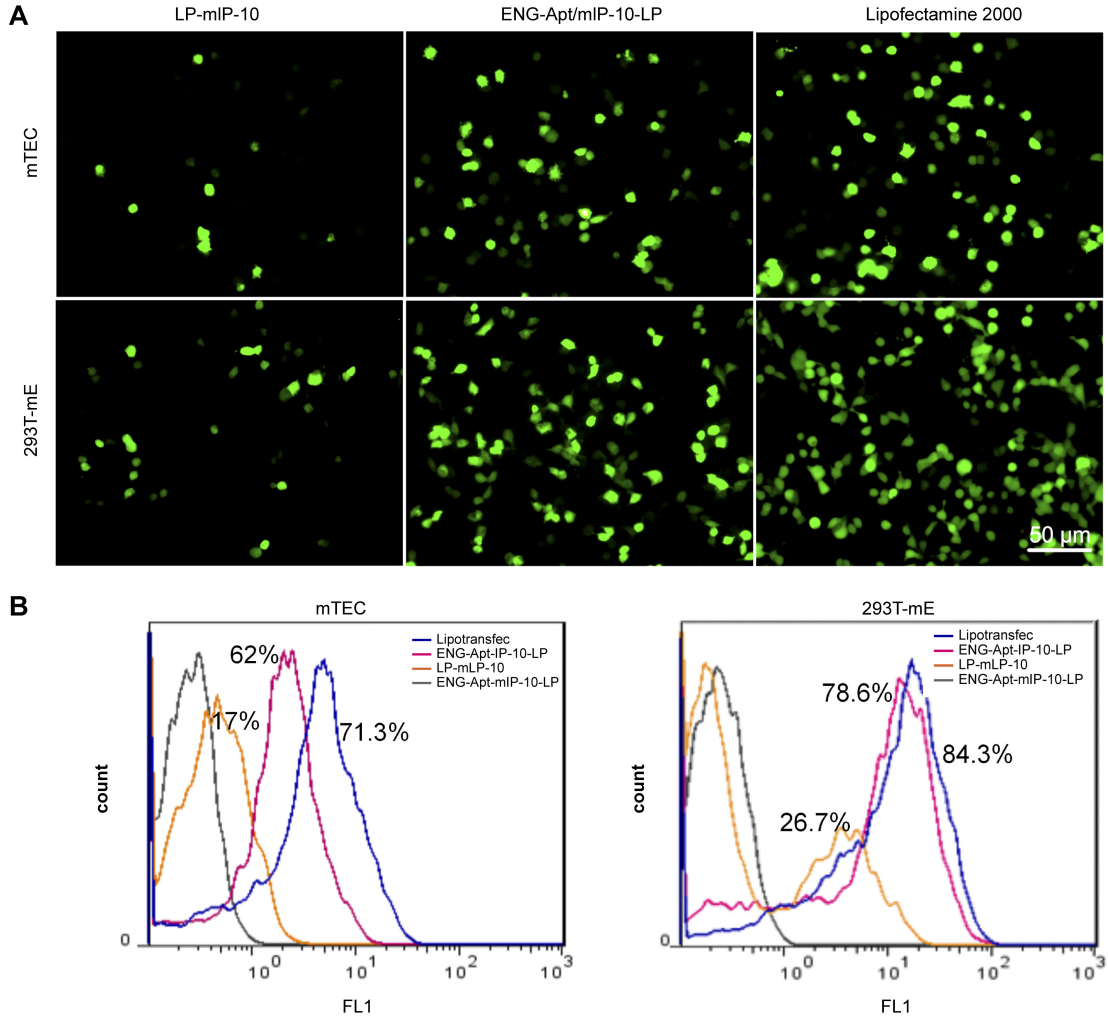


**Supplementary Figure 6: ENG-Apt/mIP-10-LP increased IP-10 expression in mTEC and 293T-mE cells. IP-10-EGFP expression in mTEC and 293T-mE cells** were observed by fluorescence microscopy. **A:** fluorescence micrographs after ENG-Apt/mIP-10-LP, LP-mIP-10 and Lipofectamine transfection into CD105-positive cells. **B:** transfection efficiency analysis of the three nanoparticles by flow cytometry.

**Supplementary Figure 7**

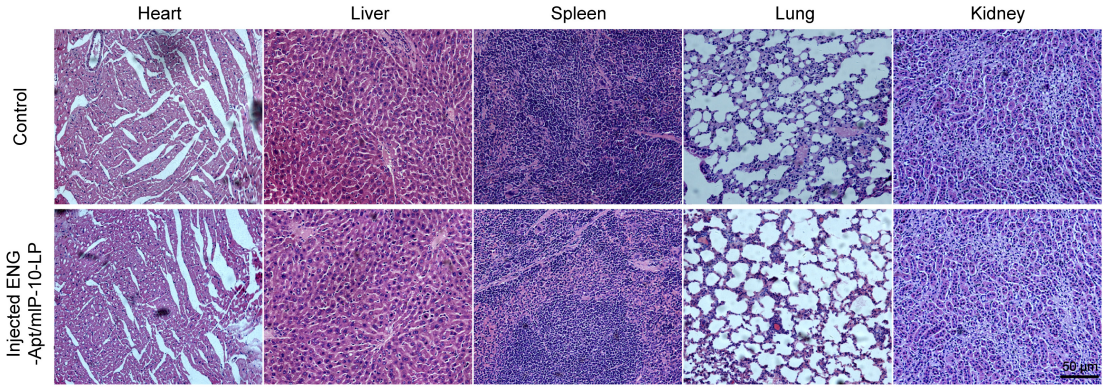


**Supplementary Figure 7: HE staining (200×)**

Heart, liver, spleen, lung and kidney of mice present no inflammatory cell infiltration or toxicity damage based on the results of HE staining.

**Supplementary Figure 8**

**A, B:** Frequency of $CD8^+$ T cells in the TIL of melanoma-bearing mice by flow cytometric analyses, and the numbers of $CD8^+$ T cells in tumor tissues with high expression of IP-10 after treatment with ENG-Apt/mIP-10-LP were significantly more than that after treatment with mIP-10-LPs.

**C, D:** ELISPOT detection showed that after treatment with ENG-Apt/mIP-10-LP nanocapsules significantly more IFN-γ–secreting cells were observed among the TILs than after mIP-10-LP treatment, with significantly fewer positive spots appearing in the PBS-treated group and the mIP-10-treated group.

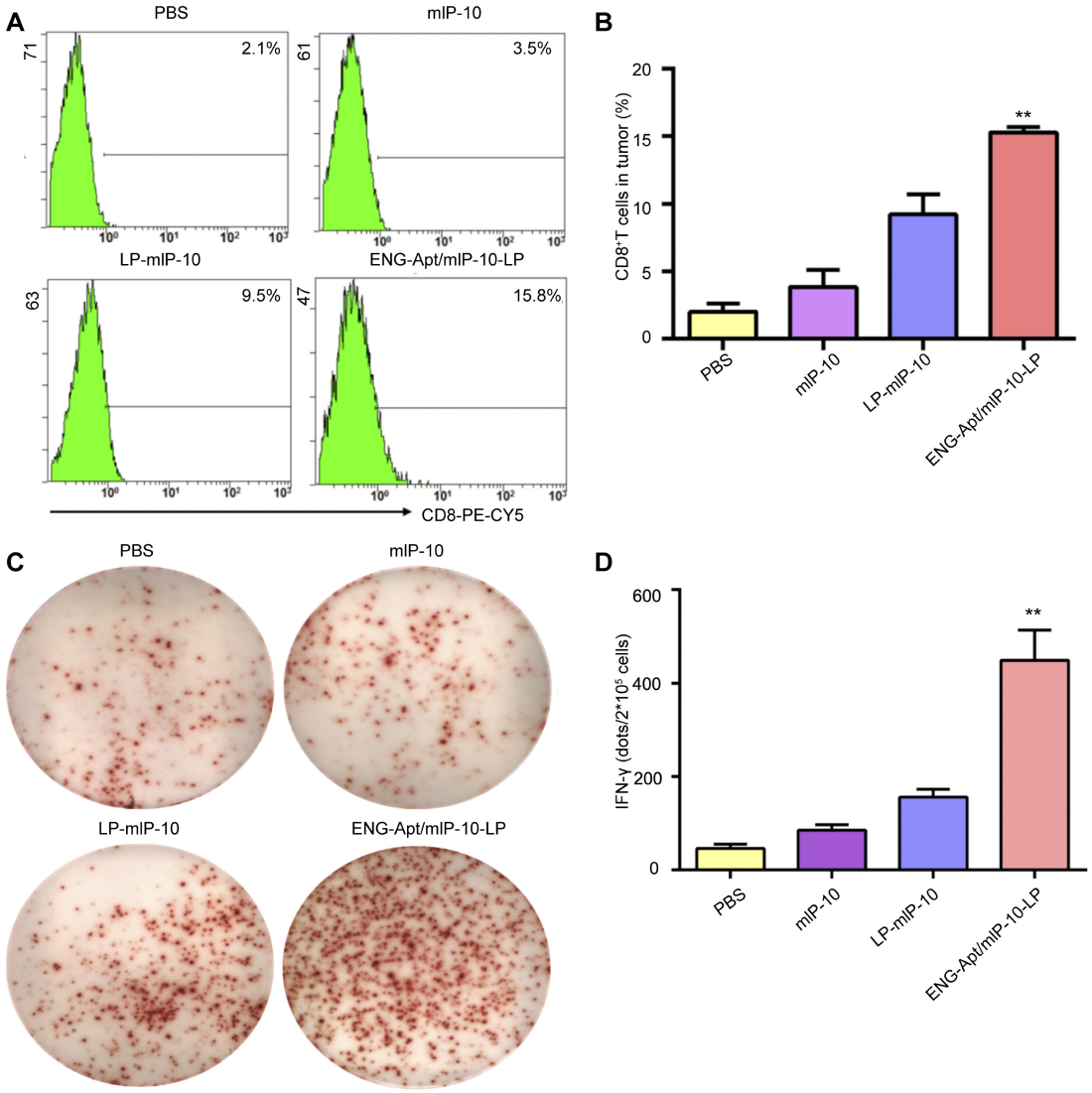


**Supplementary Figure 8: ENG-Apt/mIP-10-LP targets tumor sites and can effectively chemotaxis $CD8^+$ T to tumor sites.**

**A:** the percentage of infiltrating $CD8^+$ T cells in TIL was analyzed by flow cytometry. **B:** quantitation of $CD8^+$ T cells in TIL; **C:** the number of IFN-γ-positive spots in splenocytes by ELISPOT. **D:** comparison of statistics dots in each group and controls.

The mean ± SE of three independent experiments is shown. ** $p < 0.01$ for the comparison of ENG-Apt/mIP-10-LP group to control groups.

**Supplementary Figure 9**

Flow cytometry was used to detect myeloid-derived suppressor cell (MDSCs) in bone marrow, spleen, as well as isolated tumor-infiltrating lymphocytes (TILs) after treatment. The results showed that the percentage of MDSCs in vivo after treatment with ENG-Apt/mIP-10-LP significantly decreased, likewise, Tregs in the spleen as well as tumor infiltrating lymphocytes showed similar trends.

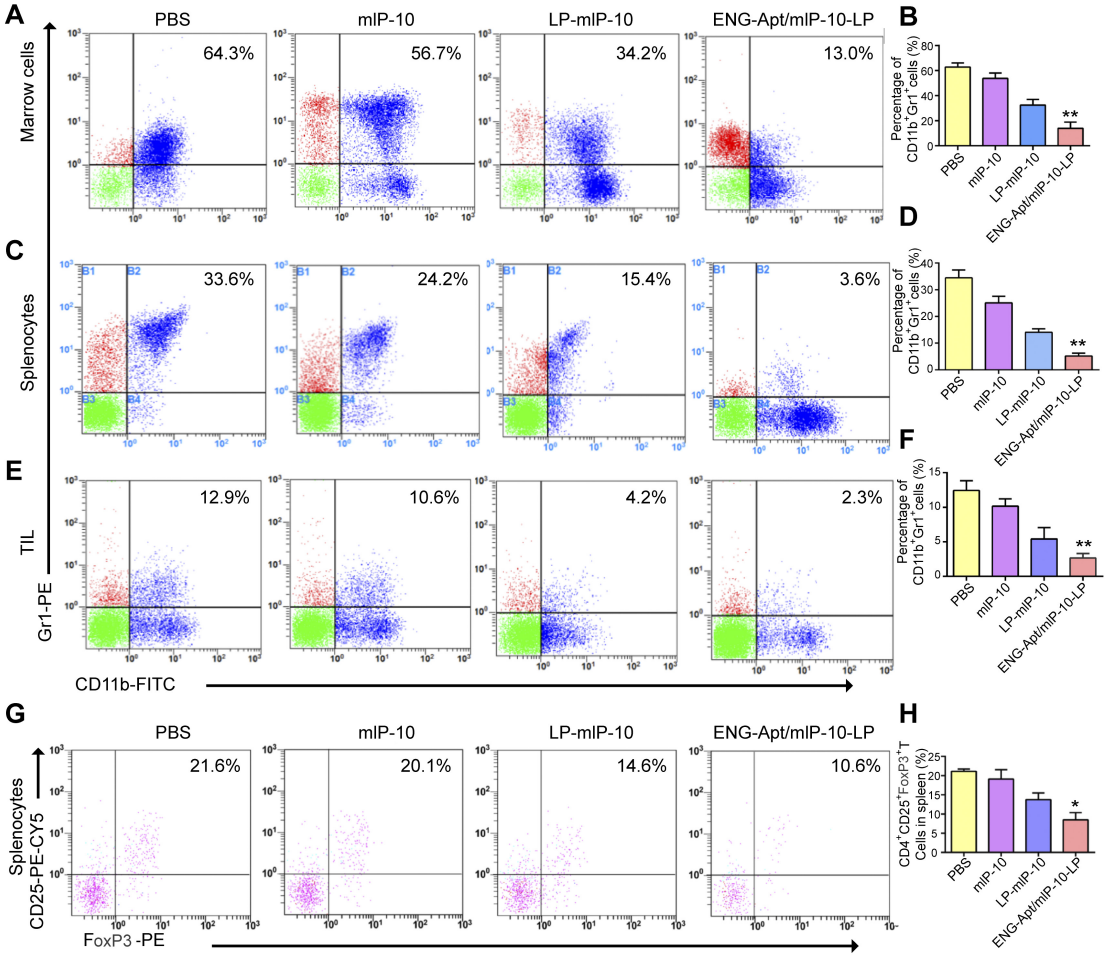


**Supplementary Figure 9:** The percentage of MDSC and Treg cells. **A, C, E:** the percentage of MDSC ($CD11b^+Gr1^+$) in marrow, splenocytes and tumor were analyzed by flow cytometry. **B, D, F:** quantitation of MDSC in marrow, splenocytes and tumor. **G:** the percentage of Treg ($CD4^+$ $CD25^+$ $FoxP3^+$) in splenocytes. **H:** quantitation of Tregs in splenocytes. All experiments were performed in triplicates and mean ± SE is shown. * $p < 0.05$; ** $p < 0.01$ for the comparison of ENG-Apt/mIP-10-LP group to control groups.

**Supplementary Figure 10**

Changes in the expression of proliferating cells nuclear antigen (PCNA) were detected via immunohistochemical staining, and the results showed that the group treated with ENG-Apt/mIP-10-LP had significantly fewer PCNA-positive cells than the group treated with mIP-10-LPs (A, C). Apoptosis in tumor tissues after treatment was further investigated by TUNEL method. Apoptosis among tumor cells after treatment with ENG-Apt/mIP-10-LP nanocapsules significantly increased and was greater than that after treatment with mIP-10-LPs (B, C).

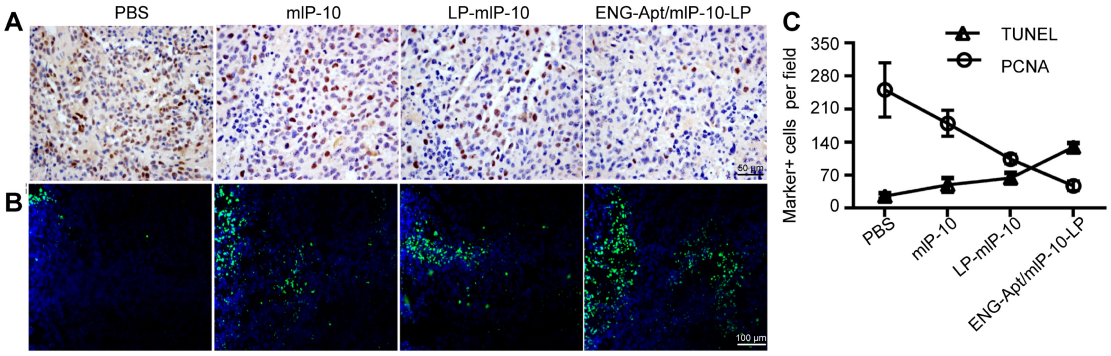


**Supplementary Figure 10: Proliferation and apoptosis of tumor cells. A:** tumor PCNA positive cells after treatment. PCNA-positive cells in each group, 400×. **B:** TUNEL assay on tumor cells' apoptosis. Apoptotic cells (green), cell nuclei labeled with DAPI (blue), 200×. Apoptotic -positive cells in each group. **C:** PCNA-positive and apoptotic-positive cells in each group. The mean ± SE of three independent experiments is shown. ** $p < 0.01$ for the comparison of ENG-Apt/mIP-10-LP group to control groups.

**Supplementary Figure 11**

Immunohistochemical staining of tumor tissues for CD31 expression illustrated a remarkably reduced tumor vascular density after treatment with ENG-Apt/mIP-10-LP nanocapsules, which was positively correlated with mIP-10 expression. The vascular density in the tumor was also lower than that in the mIP-10-LP group and 5-6 times lower than the densities in the PBS and mIP-10 groups.

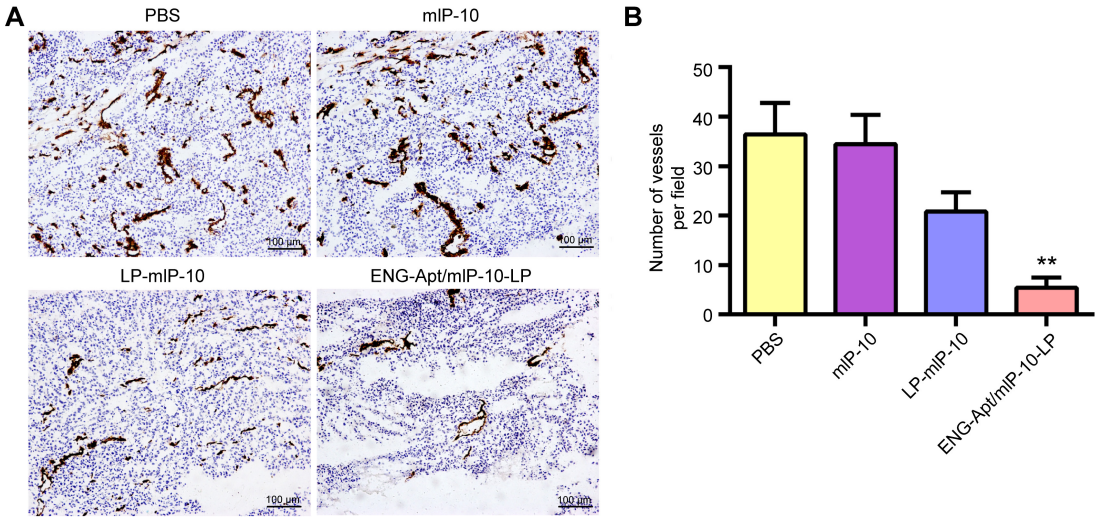


**Supplementary Figure 11: Vascular density in tumor tissue.**

**A:** Anti-CD31 immunohistochemical staining for tumor vascular density. **A:** tumor vascular density in tumor tissue, 100×. **B:** statistical comparison of CD31 positive vessels in each group. The mean ± SE of three independent experiments is shown. ** $p < 0.01$ for the comparison of ENG-Apt/mIP-10-LPgroup to control groups.